Acta Crystallographica Section D
Biological Crystallography
ISSN 0907-4449

Probing the S2 site of factor VIIa to generate potent and selective inhibitors: the structure of BCX-3607 in complex with tissue factor–factor VIIa

Raman Krishnan,* Pravin L. Kotian, Pooran Chand, Shanta Bantia, Scott Rowland and Y. S. Babu

BioCryst Pharmaceuticals, 2190 Parkway Lake Drive, Birmingham, AL 35216, USA

Correspondence e-mail: rkrishnan@biocryst.com

Received 13 February 2007
Accepted 23 March 2007

PDB Reference: TF–FVIIa–BCX-3607 complex, 2ec9, r2ec9sf.

Factor VIIa (FVIIa) is a trypsin-like serine protease in the coagulation cascade. Its complex with tissue factor (TF) triggers the extrinsic pathway of the coagulation cascade, generating a blood clot. Research programs at several centers now recognize the important roles played by TF and FVIIa in both the thrombotic and inflammatory processes associated with cardiovascular diseases. Therefore, inhibition of the TF–FVIIa complex is seen as a promising target that is key to the development of clinical candidates for various cardiovascular applications. The crystal structure of the TF–FVIIa enzyme complex has been analyzed in order to design and synthesize small-molecule inhibitors. Using structure-based drug design (SBDD), a new series of inhibitors have been discovered that demonstrate high potency against the TF–FVIIa complex while maintaining substantial selectivity *versus* other closely related serine proteases such as trypsin, thrombin, factor Xa and plasmin.

1. Introduction

The coagulation cascade has been the subject of intensive investigation over the last two decades and has been extensively reviewed (Davie *et al.*, 1991). The ability to form blood clots is vital to human survival. Thrombosis (blood-clot formation) results from a complex sequence of biochemical events known as the coagulation cascade. This chain reaction is fuelled either by one or both of two biochemical systems: the intrinsic system, in which all the components are plasma-derived, and the extrinsic system, in which the starting factor is derived from outside the blood. Recent studies have suggested that selective inhibition of the extrinsic pathway provides effective anticoagulation and low risk of bleeding compared with antithrombotic mechanisms (Szalony *et al.*, 2002).

Factor VIIa (FVIIa) and tissue factor (TF) play essential roles in the initiation of the extrinsic pathway of blood coagulation. Complex formation between FVIIa and TF dramatically enhances the catalytic activity of FVIIa (by ~10 000-fold), leading to the initiation of the extrinsic pathway. The resulting TF–FVIIa complex further activates factors IX and X to IXa and Xa, respectively. These active proteases complete the chain reaction to activate thrombin from prothrombin. In the final stage, thrombin cleaves fibrinogen to fibrin and activates platelets, the final two major components of a blood clot (Higashi *et al.*, 1994). After the formation of the blood clot, the activity of the TF–FVIIa complex is suppressed by a Kunitz-type protease-inhibitor protein tissue-factor pathway inhibitor (TFPI) which, when complexed to FXa, can directly inhibit the proteolytic activity of TF–FVIIa (Petersen *et al.*, 1996). In order to maintain the coagulation cascade in the presence of an inhibited extrinsic

Table 1
X-ray diffraction data-collection and refinement statistics.

Values in parentheses are for the outer resolution shell.

Wavelength (Å)	1.5416
Space group	$P2_12_12_1$
Unit-cell parameters	
a (Å)	69.79
b (Å)	81.41
c (Å)	125.35
Resolution (Å)	25–2.00 (2.07–2.00)
Total reflections	204170
Unique reflections	48596
Completeness (%)	99 (98)
$R_{\rm merge}$† (%)	0.079 (0.36)
$\langle I/\sigma(I)\rangle$	8.9 (3.2)
Refinement	
Resolution (Å)	25.00–2.00
Reflections used	42984
$R_{\rm cryst}$‡ (%)	24.1
$R_{\rm free}$§ (%)	28.1
R.m.s.d. bonds (Å)	0.006
R.m.s.d. angles (°)	1.58
Average *B*, all atoms (Å^2)	27.5
Average *B*, inhibitor atoms (Å^2)	21.8
Total non-H atoms	4956
Protein atoms	4688
Inhibitor atoms	35
Water molecules	224
Ca^{2+} ions	9

† $R_{\rm merge} = \sum_h \sum_i |I_{hi} - \langle I_h\rangle| / \sum_h \sum_i I_h$, where $\langle I_h\rangle$ is the weighted average intensity of the unique reflection with Miller index h that has been computed from the scaled and corrected symmetry-related observations of the reflection. The outer sum is over all unique reflections and the inner sum is over the symmetry-related observations for the reflection with Miller index h. ‡ $R_{\rm cryst}$ is calculated from 90% of the reflections used for refinement ($R_{\rm cryst} = \sum |F_{\rm obs} - F_{\rm calc}| / \sum |F_{\rm obs}|$). § $R_{\rm free}$ is calculated using the same formula from 10% of randomly selected reflections not included in the refinement process.

system, additional FXa is produced *via* the thrombin-mediated activity of the intrinsic pathway. Thus, thrombin plays a dual autocatalytic role as a procoagulant and an anticoagulant. This autocatalytic nature of thrombin generation is an important safeguard against uncontrolled bleeding and ensures that blood coagulation will proceed to completion in the presence of a threshold concentration of prothrombinase. Thus, for clinical purposes, it is most desirable to develop agents that can inhibit coagulation without directly inhibiting thrombin, but intervene in the cascade by inhibiting other steps such as FVIIa activity (Klingler *et al.*, 2002).

While tremendous progress has been made in the discovery of potent and selective inhibitors of thrombin (Balasubramanian, 1995) and FXa (Zhu & Scarborough, 2000), it is only recently that there have been focused efforts towards the discovery of inhibitors of the extrinsic pathway. The market value for such drug candidates has been estimated to be in excess of $1 billion (Stagnitti, 2006). Symptoms resulting from an abnormal blood clot can cause ischemic stroke, unstable angina, deep-vein thrombosis, pulmonary embolism and acute myocardial infarction. Current therapies, such as warfarin, heparin and related sulfated polysaccharides, are only marginally effective in treating these symptoms. A specific inhibitor of TF–FVIIa with a favorable pharmacological profile leading to an oral drug would have tremendous value in cardiovascular treatment.

The first crystal structure of the blood-coagulation FVIIa complexed with soluble tissue factor (sTF) was reported by Banner *et al.* (1996). The crystal structures of FVIIa without TF (Kemball-Cook *et al.*, 1999; Pike *et al.*, 1999; Eigenbrot *et al.*, 2001) and of ternary complexes of several sTF–FVIIa–inhibitor complexes (Zhang *et al.*, 1999; Dennis *et al.*, 2000; Klingler *et al.*, 2003; Parlow, Case *et al.*, 2003; Parlow, Dice *et al.*, 2003; Parlow, Kurumbail *et al.*, 2003*a*,*b*; Parlow, Stevens *et al.*, 2003; South *et al.*, 2003; Kadono *et al.*, 2004; Kadono, Sakamoto, Kikuchi, Oh-eda, Yabuta, Koga *et al.*, 2005; Kadono, Sakamoto, Kikuchi, Oh-eda, Yabuta, Yoshihashi *et al.*, 2005; Kohrt *et al.*, 2005) determined recently have given us a very good understanding of the nature of the active site and the interactions of model compounds with this enzyme complex. All these crystal structures provide a strong structural basis for the SBDD approach (Rowland, 2002) to develop selective small-molecule active-site inhibitors for TF–FVIIa.

Using the SBDD strategy, we set out to study the active site of sTF–FVIIa and synthesize an effective inhibitor as the first step in the development of a successful cardiovascular drug. This manuscript describes the enzyme–inhibitor structural complexes used in optimizing the key interactions in the active site. Our design efforts culminated in a nanomolar inhibitor that is selective for FVIIa.

2. Materials and methods

2.1. Compound synthesis and inhibition assay

The small-molecule TF–FVIIa inhibitors ('BCX-#') used in these studies were synthesized at BioCryst Pharmaceuticals Inc. Details of the synthesis and structure–activity relationships will be reported elsewhere (Kotian *et al.*, 2007). Inhibition activities for human TF–FVIIa and related serine proteases were measured using chromogenic substrates.

2.2. Crystallization

The FVIIa used for crystallization was purchased from NHS Hospital Specialties, Hackensack, NJ, USA (NOVO7) and used without further purification. A 15–50% molar excess of BCX compounds was dissolved and added to the FVIIa solution and left to thaw on ice. The inhibited FVIIa was stored in a cold room for 12 h to complete FVIIa–BCX-# complex formation. The ternary complexes of the FVIIa–BCX-# compounds were made by adding a 10% excess of sTF [3.1 mg ml^{-1} in 20 m*M* Tris–HCl pH 7.5, 0.02%(*w*/*v*) NaN_3] from Sunol Molecular Corp., Miramar, FL, USA to this solution of inhibited FVIIa. The ternary complexes were concentrated after 12 h using a 50 kDa molecular-weight cutoff Centricon filter in a refrigerated centrifuge (277 K). They were then diluted tenfold with 20 m*M* Tris–HCl pH 7.5, 2 m*M* $CaCl_2$ buffer and concentrated three times in order to remove excess BCX compound and sTF. The final concentration of sTF–FVIIa–BCX-# was 15 mg ml^{-1} in FVIIa. Optimal crystal growth was observed at room temperature in a 2 µl hanging drop comprised of 1 µl protein solution and 1 µl

precipitant [14%(*w*/*v*) PEG 4K, 0.1 *M* $MgCl_2$, 0.1 *M* ADA buffer pH 6.5] equilibrated over 0.5 ml well solution.

2.3. Data collection

X-ray diffraction data were measured at BioCryst Pharmaceuticals Inc. using an R-AXIS IV^{++} imaging-plate detector and radiation generated from a Rigaku RU-200 rotating-anode generator operating at 5 kW power with a fine-focus filament (0.3 × 3.0 mm). The Cu $K\alpha$ radiation was focused using Osmic confocal mirrors (Rigaku MSC). Autoindexing and processing of the measured intensities were carried out using the *CrystalClear* software package (Pflugrath, 1999). All crystals used for data collection were passed through a cryoprotectant solution containing 12% glycerol and then flash-frozen *in situ* using an X-Stream cryostat (Rigaku MSC). Data were collected at a crystal-to-detector distance of 120 mm, with an oscillation angle of 1° and an exposure time of 2 min per frame (Table 1). Typically, a 100° rotation was sufficient to generate complete data sets. Data collection and processing were performed using the *CrystalClear* software package. The crystals of the sTF–FVIIa–BCX-# ternary complexes are orthorhombic, with one molecule per asymmetric unit. The overall R_{merge} was usually in the range 10–11% for these data sets. The crystals of the ternary complexes belong to the orthorhombic crystal system, with space group $P2_12_12_1$, and are isomorphous to the previously reported D-Phe-Phe-Arg-(chloromethyl ketone) (DFFR) inhibited sTF–FVIIa crystals (Banner *et al.*, 1996; PDB code 1dan).

				IC_{50} (μ*M*)				Selectivity (IC_{50}) ratio		
BCX-#	Resolution (Å)	R_1	R_2	FVIIa	Try	Thr	FXa	Try/ FVIIa	Thr/ FVIIa	FXa/ FVIIa
2	2.8	H	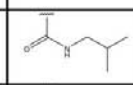	0.120	0.17	64.00	103.00	1.5	533.3	858.3
3A	2.4	-OH	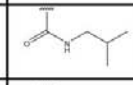	0.067	0.39	50.00	50.00	5.8	746.3	746.3
3B	2.8	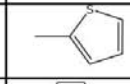	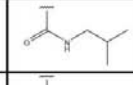	0.010	0.32	6.12	0.41	32.4	612.0	41.0
3C	—	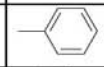	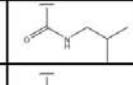	0.098	0.42	11.82	0.35	4.3	120.6	3.6
3D	2.7		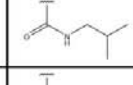	0.021	0.57	8.51	1.75	27.1	405.2	83.3
3E	2.3	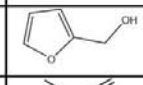	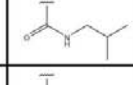	0.024	0.77	50.00	0.15	32.1	2083.3	6.3
3F	2.5	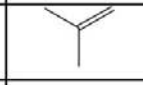	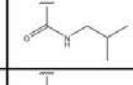	0.013	0.53	17.90	1.17	40.8	1376.9	90.0
3G	2.1	-OH_2	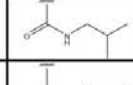	0.030	0.152	13.50	2.30	5.1	450.0	76.7
4	2.4	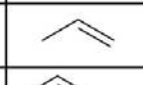	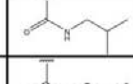	0.009	0.470	9.40	1.65	52.2	1044.4	183.3
3607	**2.0**	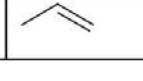	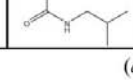	**0.004**	**61.2**	**5.3**	**0.34**	**15300.0**	**1325.0**	**85.0**

(*a*)

				IC_{50} (μ*M*)				Selectivity (IC_{50}) ratio		
BCX-#	Resolution (Å)	R_1	R_2	FVIIa	Try	Thr	FXa	Try/ FVIIa	Thr/ FVIIa	FXa/ FVIIa
5*	—		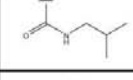	8.6	—	—	—	—	—	—
6	—		H	0.19	—	—	—	—	—	—
7	—	H	H	5.72	0.89	16.70	79.27	0.16	2.9	13.9

(*b*)

Figure 1
(*a*) BCX compounds with various substitutions on ring *A*, with IC_{50} values for FVIIa and selectivity. For clarity and brevity, discussion is confined in this paper to the effect that different substituents on the *A* ring, which interacts in the S2 pocket, had on the binding and selectivity of FVIIa and other homologous serine proteases in the blood-coagulation pathway. OH_2 for compound BCX-3G indicates a hydroxyl group at position 2 (Fig. 2). (*b*) Loss of binding to FVIIa upon losing one or more substituents on the core molecules. The asterisk for compound 5 indicates the absence of carboxylate on ring *B* in this compound. Try, trypsin; Thr, thrombin; Fxa, factor Xa.

2.4. Structure determination

Ther *CNX* suite of programs (Brünger *et al.*, 1998) was used for all computations and analyses. Initial coordinates and stereochemical features for the inhibitor portion were prepared using the builder module of *QUANTA* (Accelrys). Structure solution of the ternary complexes began with a rigid-body rotation–translation refinement using the coordinates of sTF–FVIIa (from PDB entry 1dan) minus the inhibitor and water molecules, with the temperature factor for all atoms set to an average *B* factor (30 Å^2) for the entire complex. The refinements generally started at an *R* factor of 32–35% (R_{free} = 34–36%). After the convergence of the rigid-body calculations at an *R*-factor of 28–30% (R_{free} = 31–33%) and a round of temperature-factor/coordinate refinement, including the water molecules (restricted to 100 and picked using the automatic water-picking routine implemented in *CNX*), the *R* factor fell to 24–26% (R_{free} = 28–29%). The inhibitor was easily located and modelled in the $(2|F_o| - |F_c|)$ and $(|F_o| - |F_c|)$ electron-density maps calculated at this stage. For all the inhibitor complexes, the computation was deemed sufficient and was stopped since the difference electron-density

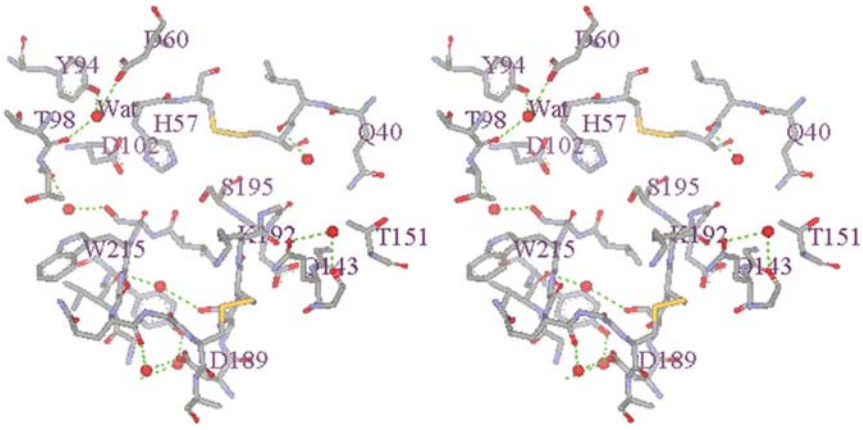

Figure 2
Residues of FVIIa within 6 Å of BCX-3607 are used to depict the active site. FVIIa is shown in stick representation, with key residues labelled using chymotrypsin numbering. A structurally conserved water molecule (Wat) binds in the S2 subsite (Asp60, Thr98, Tyr94).

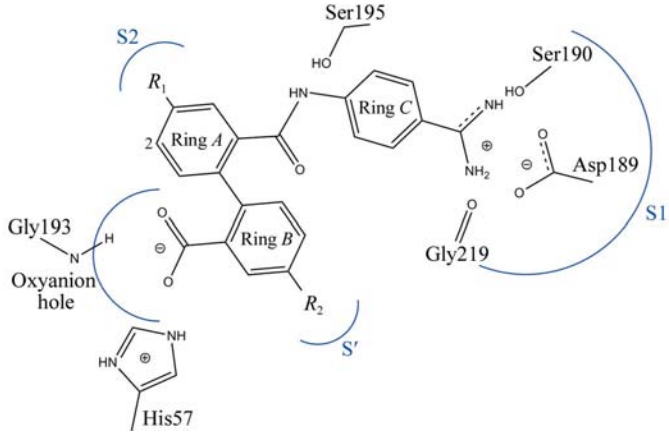

Figure 3
Binding mode for BCX-# inhibitors in the active site of the sTF–FVIIa complex.

maps were clear enough and allowed us to interpret the binding and conformation of the inhibitor unambiguously. The structures revealed that the rigid core of the BCX-# inhibitors bound exactly the same way to the active site irrespective of the R_1 group. As we did not expect any change in the inhibitor conformation with continued refinement, these ternary complex structures were not refined any further. As they were used only as intermediate checkpoints to steer our SBDD efforts in the right direction, it is beyond the scope of this paper to provide details of the data collection/refinement of all the complexes listed in Fig. 1(*a*).

However, the crystal structure of the BCX-3607 complex was refined to completion as it was the successful end point of our SBDD efforts. The crystal structure of the sTF–FVIIa–BCX-3607 complex is also the best representative of all of the BCX complexes (Table 1). Thus, a second round of refinement, combined with temperature-factor refinement for the BCX-3607 complex, occupancy refinement for the 224 water molecules and positional refinement of all the atoms, reduced the final *R* factor to 24%. A Ramachandran map calculated using *MOLPROBITY* (Lovell *et al.*, 2003) showed that 93.8% of all the residues were in favored regions (98.6% were in allowed regions). The protein structure is very similar to that of the sTF–FVIIa complex (PDB code 1dan); the r.m.s.d. of all the backbone atoms after superposition was only 0.51 Å.

3. Results and discussion

3.1. Structure-based drug design

The numbering of the FVIIa and other serine-protease residues used is based on topological equivalence with chymotrypsin (Banner *et al.*, 1996; Bode *et al.*, 1989). Since the overall conformation of the active site as well as the position of the catalytic site residues is very similar in thrombin, FVIIa, FIXa and FXa, developing a selective sTF–FVIIa inhibitor was a challenge. However, there is a wealth of structural information available regarding the design of highly specific small-molecule active-site inhibitors for homologous serine proteases such as thrombin (Balasubramanian, 1995) and FXa (Zhu & Scarborough, 2000). A careful study of these indicate that high selectivity and specificity were achieved by utilizing the subtle structural differences in the S2, S3 and, in a few cases, the S′ pockets of these enzymes. All the inhibitors reported in this manuscript contain a benzamidine moiety, similar to the majority of inhibitors targeted to bind at the active site of coagulation enzymes such as factor Xa (FXa), thrombin and factor IXa (FIXa).

In the three coagulation proteases thrombin, FXa and FVIIa, only the S2 pocket of FVIIa is relatively open and has a negative potential owing to the presence of Asp60 at its narrow end (Fig. 2). FXa has a Tyr residue at position 60 and its S2 site is practically occluded by Tyr99. Thrombin, on the other hand, has a bulky hydrophobic lid comprising of the 60s insertion loop, which has a number of aromatic residues which cover the S2 pocket. The S′ sites are the pockets N-terminal to the scissile bond of the substrate and play an important role in substrate recognition. The S1′ and S2′ sites of FVIIa are lined with Cys42 and His57 and more distantly with Leu41 and with Gly193 and Lys192, respectively. Further downstream of these residues is the hydrophobic pocket formed by Thr151, Gln143 and Gln140.

Initially, the first set of compounds were designed to provide a rigid core that was easy to synthesize and that would enable us to add various groups to probe the S2 and S′ pockets of the enzyme. Beginning with benzamidine docked in the S1 pocket, we decided to add a phenyl ring (ring *A*, Fig. 3) with an amide linker, which acted as a central scaffold to project the substituents appropriately into the S2 site. A phenyl ring was deemed appropriate after studying the sTF–FVIIa–DFFR (PDB code 1dan) and sTF–FVIIa–5L15 (PDB code 1fak) ternary complexes, as the S2 apolar site is occupied by a

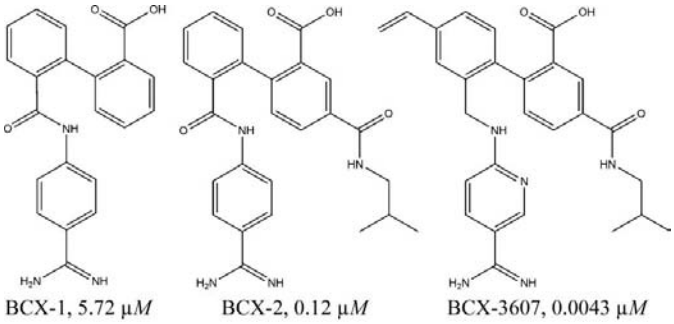

Figure 4
Chemical structures of the BCX inhibitors at various stages of SBDD. All the structures reported use the core of BCX-1 with modifications at R_1. The numbers shown are the IC_{50} values for the sTF–FVIIa complexes.

hydrophobic phenylalanine side chain and a disulfide bridge, respectively, in these crystal structures. Based on our own modeling and docking studies (using *MOE*; Chemical Computing Group Inc., Montreal, Canada; http://www.chemcomp.com), we added another rigid planar group (ring *B*) to which we could add groups to probe the S′ sites. The negatively charged carboxylic acid group was designed to interact with His57 or Lys192 of FVIIa and to occupy the oxyanion hole. With these two rings in place, consistent manual and automated docking results plus structural work using the compounds BCX-2, BCX-3A and BCX-3B (Fig. 1*a*) led us to infer that our core groups rings *A*, *B* and *C* bound in the active site of FVIIa in exactly the same way irrespective of the R_1 and R_2 groups added onto them. As expected, the benzamidine group acted as an ideal arginine surrogate and formed the anchor point for all these 'BCX-#' inhibitors. The positively charged amidino group of the benzamidine moiety formed a symmetric salt bridge with the side-chain carboxylate of Asp189 and was further stabilized by hydrogen bonds to the main chain of Gly219 and the side chain of Ser190 in the S1 pocket. It was confirmed that the carboxylate group on ring *B* bound on the inside of the active site interacted with the catalytic His57 instead of the Lys192 residue, the side chain of which was exposed to the solvent. Armed with these facts, we were ready to probe the S2 site with various substituents in search of a selective potent inhibitor. BCX-1 (Fig. 4) was the core structure of all the BCX inhibitors. The compound displays some selectivity toward FXa and thrombin, even when devoid of groups binding in the S2 or S′ pockets. The

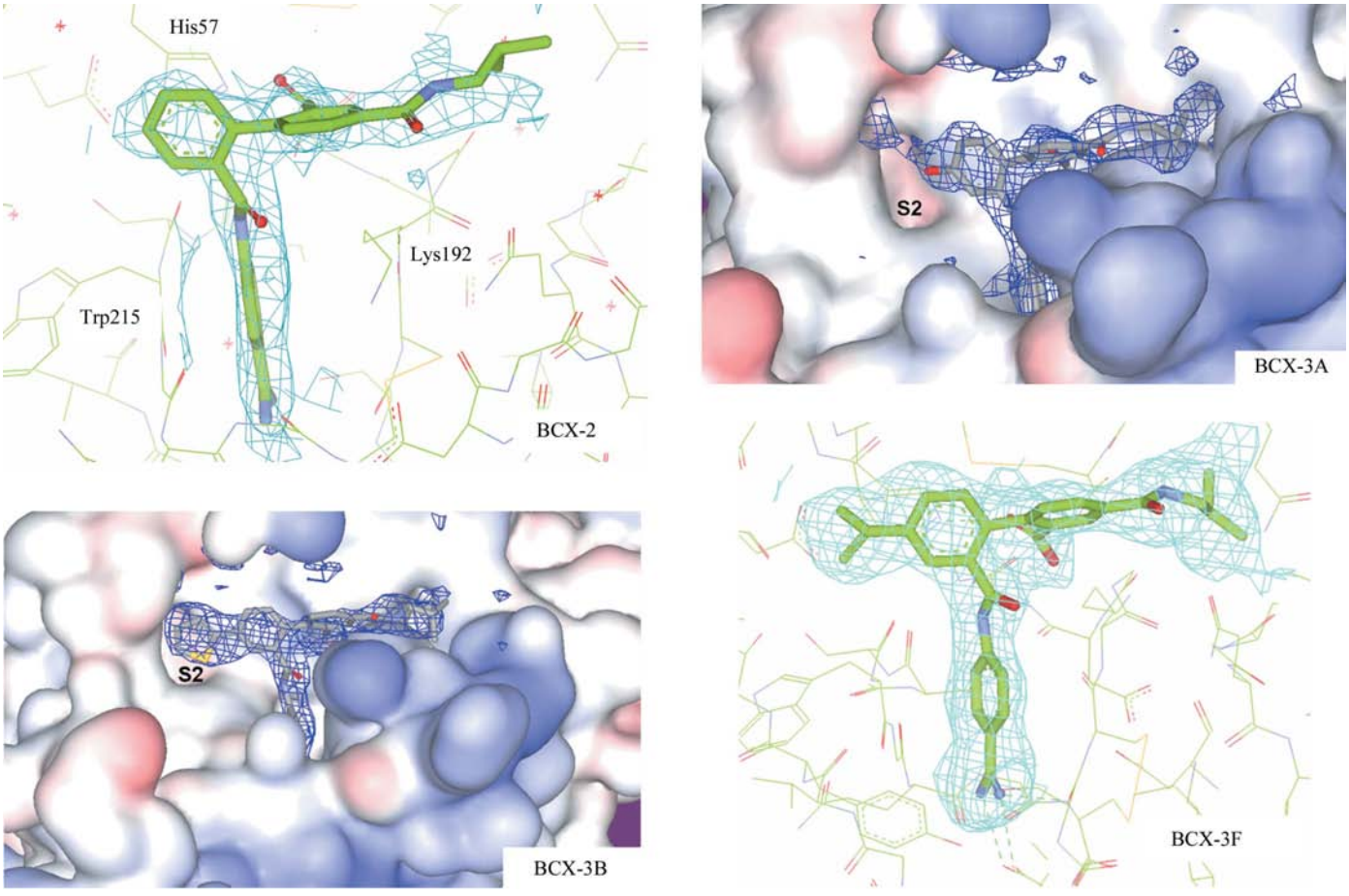

Figure 5
BCX compounds from Fig. 1 bound at the active site of the FVIIa–sTF complex. The labels at the bottom of each figure correspond to the compound No. in Fig. 1(*a*). The pictures indicate the progressive improvements made using crystallography to design better inhibitors for FVIIa. The surface representations of the FVIIa active site, shown looking into the S2 pocket, show that the thiophenyl group is a good fit. The quality of the crystal structures can be inferred by difference ($|F_o| - |F_c|$) electron-density contours drawn at the 2σ level on the inhibitors, without the inclusion of the BCX-# compounds.

next compound BCX-2 (Fig. 4) in the series has an isopropyl group that binds in the S′ sites of these proteases. Steric hindrance at the S2 site for both FXa and thrombin and undesirable contacts at the S′ site with the main-chain atoms of Gly40 and the side-chain atoms of Gln151 for FXa seem to result in reduced binding compared with that of BCX-1 to thrombin and FXa. In the case of trypsin, the isopropyl group makes short contacts with Tyr151 and His40 side-chain atoms in the S′ site. The presence of a polar side chain also renders this cavity more hydrophilic compared with that of FVIIa. Also, the alkyl side chain of Lys192 (Glu or Gln in other serine proteases) stacks below ring *B*, contributing to the hydrophobic interactions in FVIIa.

Starting with a hydroxyl, many moieties of different chemical composition were synthesized for the R_1 group (Fig. 5). Among this 'BCX-#' group, a thiophene group at R_1 seemed to give the best binding to FVIIa (BCX-3B). Increasing the size and changing the charge by adding further groups onto the five-membered ring at the R_1 position did not improve the binding significantly. Also, careful analysis of crystal structures of these BCX inhibitors complexed to sTF–FVIIa revealed that the thiophene ring at the S2 position was an ideal fit. Phenyl or heterocycle rings fared no better than adding small chemical moieties (BCX-3C, BCX-3E) onto the five-membered ring.

We realised that compounds with a bulky hydrophobic group at the R_1 position that reached deep into the FVIIa S2 pocket also bound better in the active site of FXa. BCX-3B and compounds with smaller R_1 groups (BCX-3A, BCX-3F) that bound only at the more widely open end of the S2 pocket (Fig. 6) were more selective for FVIIa than FXa. The poor binding of the latter type of compounds to FXa is a consequence of the unfavorably short contacts to the side-chain atoms of the Tyr99 residue of FXa. However, when the R_1 groups are hydrophobic and planar they can stack behind the tyrosine side chain, leading to better binding to FXa and resulting in less selective compounds. BCX-3F, BCX-4 and BCX-3607 were synthesized as a result of this important observation. Enzyme-binding assays revealed that the same order of inhibition could be achieved by substituting the bulky thiophene ring by a smaller alkyl or vinyl group (Figs. 1*a* and 5).

Compound BCX-3E was designed to interact in the S2 pocket by displacing the structurally conserved water bound to Asp60, the Tyr98 side-chain atoms and the carbonyl O atom of Thr98, leading to greater selectivity and more potent FVIIa inhibitors. However, the hydroxyl group (of the CH_2OH) on the thiophene ring weakly hydrogen bonded to this water molecule instead of replacing it. We inferred that an amino group in this position fared no better in this aspect, as the IC_{50} toward FVIIa was very similar to that of BCX-3E.

BCX-5, BCX-6 and BCX-7 are truncated versions of BCX-4; the IC_{50} data in Fig. 1(*b*) clearly indicate the loss of binding activity with each individual modification. BCX-3607 is the result of optimizing BCX-4 by removing the carbonyl O atom from the peptide linker between rings *A* and *C* and changing the P1 group benzyl ring to a heterocyclic ring by replacing a C atom by an N atom in the *meta* position to the amino groups. The latter change was made to increase the solubility of the parent compound in order to improve its pharmacological properties. The rotational freedom gained by the benzamidine group and the reduction in hydrophobicity resulted in improving binding to FVIIa by two orders (Fig. 1*a*).

Figure 6
A schematic representation of sTF–FVIIa in complex with BCX-3607. FVIIa is shown in orange (heavy chain) and blue (light chain). The two domains of TF are shown in red (1) and green (2), respectively. BCX-3607 is shown as a space-filled model.

3.2. Crystal structure of sTF–FVIIa–BCX-3607

BCX-3607 is a noncovalent, reversible and competitive inhibitor of the sTF–FVIIa complex. It physically blocks the active site in the catalytic domain of FVIIa and prevents its natural substrate FX from binding and undergoing catalytic cleavage. BCX-3607 is bound to the substrate-binding cleft occupying the S1, S2 and S′ sites of the catalytic domain of FVIIa (Fig. 6). The $2|F_o| - |F_c|$ electron-density map for BCX-3607 is complete and continuous over all the atoms except for the terminal atoms of the isopropyl group (Fig. 7*a*). The central ring *A* makes interplanar angles of 70° and 64° with the benzamidine (*C* ring) and *B* ring, respectively, while the *B* ring

Table 2
Comparison of BCX-3607 and P5B: binding and selectivity for FVIIa.

Compound	IC_{50} (μM)	TF–FVIIa/thrombin	TF–FVIIa/FXa
BCX-3607	0.004	1325	85
P5B	0.034	6	1250

is almost perpendicular to the *C* ring (87°). A total of 444 Å^2 of solvent-accessible surface area is buried in FVIIa–BCX-3607 interaction. In addition to the four hydrogen bonds in the S1 pocket (two with Asp189 and one each with Ser190 and Gly219), BCX3607 partakes in three other direct hydrogen-bonding interactions with FVIIa, a hydrogen bond with the Ser195 terminal hydroxyl and two hydrogen bonds with the His57 side chain and the Gly193 main chain at the oxyanion hole, respectively (Figs. 7*a* and 7*b*).

The central *A* ring stacks on top of the catalytic His57 (closest contact 3.40 Å), with the vinyl group at R_1 positioned at the entrance to the S2 pocket, with contacts to the Thr98 (>4.2 Å), Thr99 (>3.9 Å) and Trp215 (>3.8 Å) side-chain atoms. The vinyl group is perpendicular in its orientation with respect to the Phe group of the covalent D-Phe-Phe-Arg-(chloromethyl ketone) complex with sTF–FVIIa (Fig. 8). The *B* ring provides a scaffold for the carboxylic group and the R_2 group and stacks on the side-chain atoms of Lys192. The R_2 substituents on the *B* ring extend into the S′ pockets, filling in the shallow hydrophobic cavity lined by the Leu41, Gln143 and Gln140 residues, and adopt a conformation that allows maximum van der Waals interactions.

There are no water molecules that interact directly with the BCX-3607 molecule. However, there are three water molecules at the bottom of the S1 pocket. These form a water bridge between the OD1/OD2 atoms of Asp189 and the hydroxyl group of Ser190 and residues Tyr228, Ala183, Gln217 and Val227 to stabilize their side-chain conformations. They are a part of the structurally conserved water network found in sTF–FVIIa–inhibitor complexes.

It is beyond the scope of this paper to compare and contrast all the small-molecule active-site inhibitors of FVIIa reported to date. For an excellent review, the reader is referred to Lazarus *et al.* (2004). However, we have compared another FVIIa inhibitor with BCX3607 to illustrate how SBDD strategies can lead to small molecules which could bind in different ways to achieve similar binding and selectivity towards FVIIa. Fig. 8 illustrates the structural similarities and differences between BCX-3607, P5B (PDB code 1wun; Kadono *et al.*, 2005), DFFR (1dan) and their mode of interaction with FVIIa. P5B and DFFR use the S1, S2 and S3 sites, while BCX-3607 binds to the S1, S2 and S′ sites. Table 2 lists the binding constants and selectivity for P5B and BCX-3607 against thrombin and FXa. The amide group of P5B binds in the S2 site, with the amino group replacing the structurally conserved water molecule and hydrogen bonding to Tyr94, Thr98 and Asp60 (Fig. 8). Use of a peptide spacer group after the P1 benzamidine and the flexible glutamamide group enable P5B to reach into the S2 site to successfully replace this water molecule (Fig. 7), in contrast to BCX-3E, which could only form a weak hydrogen bond to this water. P5B does not interact with the catalytic triad in the active site, unlike the

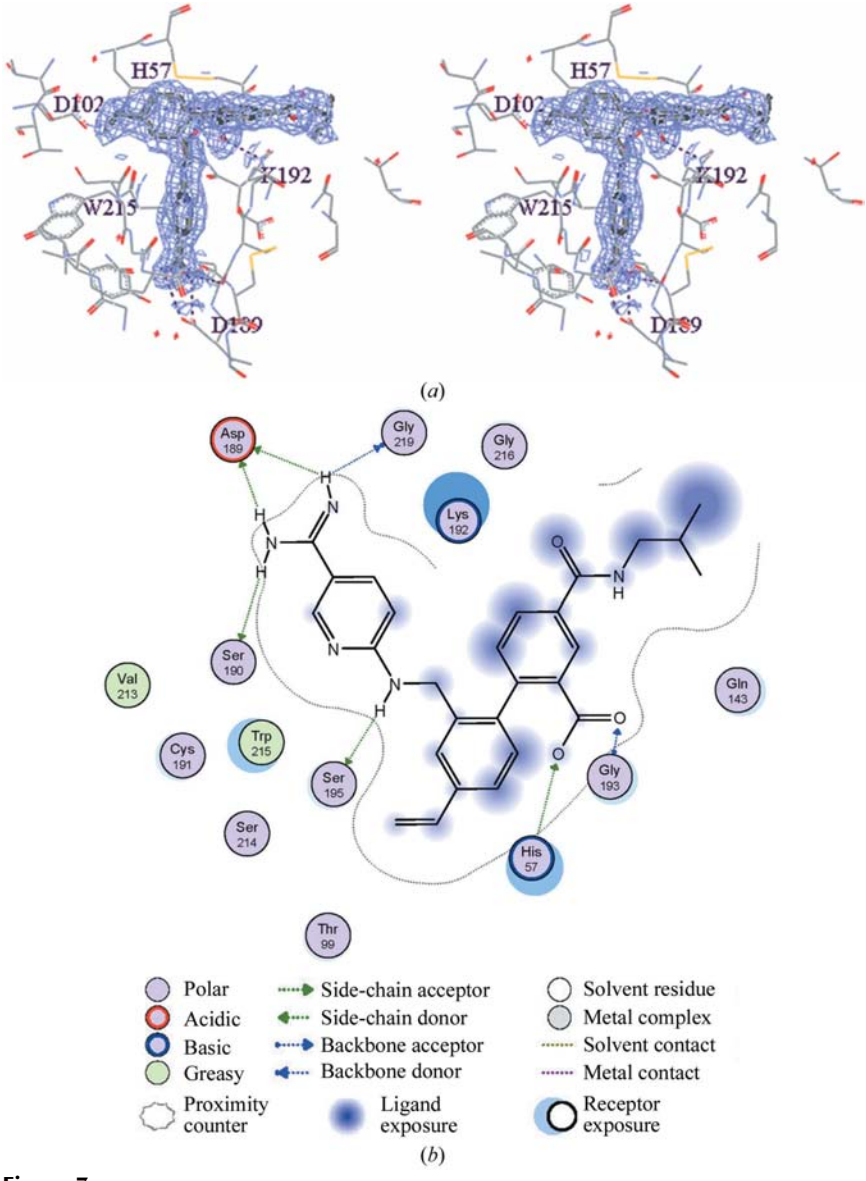

Figure 7
(*a*) BCX-3607 bound in the active site of FVIIa (thin lines). The $2|F_o| - |F_c|$ electron-density map is contoured over the inhibitor at the 1σ level with hydrogen bonds in dotted black lines. (*b*) A schematic representation of the BCX-3607–FVIIa interactions drawn using *MOE*.

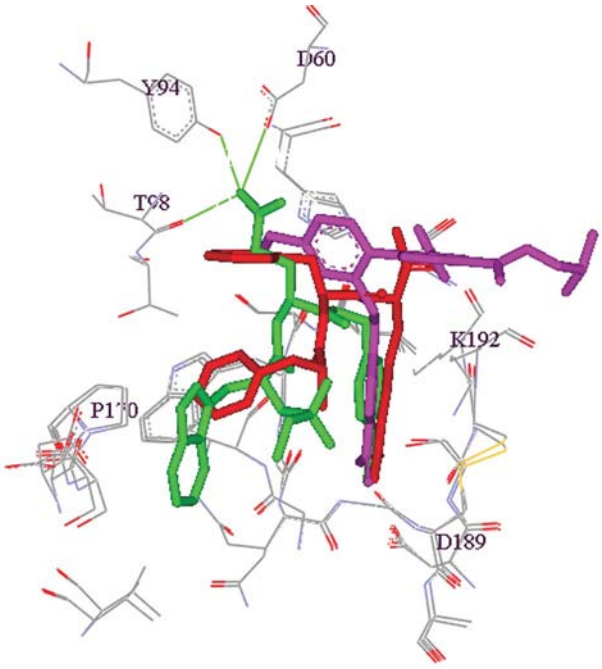

Figure 8
Crystal structures of sTF–FVIIa complexes superposed in the active-site region. BCX-3607 (magenta; PDB code 2ec9) binds in the S1, S2 and S′ pockets. DFFR-chloromethylketone (red; PDB code 1dan) is a covalent inhibitor which binds in the S1, S2 and S3 pockets. P5B (green; PDB code 1wun) binds in the S1, S2 and S3 sites. It has an amide group binding in the S2 subsite. The amino group of this amide replaces a structurally conserved water molecule to form three hydrogen bonds (green lines) to residues Tyr94, Thr98 and Asp60 of FVIIa. The amino-acid residues of FVIIa (1dan) have been omitted for the sake of clarity; also, only the residues from 1wun are shown in the S2 subsite.

covalent irreversible inhibitor DFFR. However, BCX-3607 forms hydrogen bonds to His57 and Ser195. The bulky naphthalene group at the P3 position of P5B was shown to bind to the S2 site of thrombin using modeling studies (Kadono *et al.*, 2005), resulting in rather low selectivity (Table 2). While their binding to FVIIa is roughly of the same order, the selectivity profiles of BCX-3607/P5B are complementary to one another for FXa/thrombin enzymes (Table 2). Choosing different substrate-binding sites for inhibitor interactions during SBDD enables one to fine-tune the selectivity to specific enzymes within the same family. The majority of the small-molecule active-site inhibitors of FVIIa similar to P5B and BCX-3607 have a benzamidine or a similar positively charged group at the P1 position. The ionic charge and polar functionality found in these inhibitors prevent permeability through membranes, resulting in poor oral absorption. Replacing these charged P1 groups with less basic groups or using a prodrug strategy would be the next necessary step before these inhibitors become successful oral drugs.

4. Conclusion

Our goal was to develop a selective small-molecule inhibitor(s) using SBDD for TF–FVIIa, the initiator of the extrinsic pathway. We have developed a 4.3 nm inhibitor from a 5.72 μ*M* compound using SBDD in conjunction with medicinal chemistry synthesis. Correlating both structure and activity for many intermediate compounds was subsequently clear-cut as the core of all 'BCX-#' compounds binds similarly within the active site of FVIIa. Thus, we could accurately probe and model groups into the S2 site to finally synthesize BCX-3607, an effective inhibitor of the extrinsic pathway.

We thank Dr Dion D. D. Hepburn for useful discussions and meticulous corrections to this manuscript.

References

Balasubramanian, B. N. (1995). *Bioorg. Med. Chem.* **3**, 999–1123.
Banner, D. W., D'Arcy, A., Chene, C., Winkler, F. K., Guha, A., Konigsberg, W. H., Nemerson, Y. & Kirchhofer, D. (1996). *Nature (London)*, **380**, 41–46.
Bode, W., Mayr, I., Baumann, U., Huber R., Stone, S. R. & Hofsteenge, J. (1989). *EMBO J.* **8**, 3467–3475.
Brünger, A. T., Adams, P. D., Clore, G. M., DeLano, W. L., Gros, P., Grosse-Kunstleve, R. W., Jiang, J.-S., Kuszewski, J., Nilges, M., Pannu, N. S., Read, R. J., Rice, L. M., Simonson, T. & Warren, G. L. (1998). *Acta Cryst.* D**54**, 905–921.
Davie, E. W., Fujikawa, K. & Kisiel, W. (1991). *Biochemistry*, **30**, 10363–10370.
Dennis, M. S., Eigenbrot, C., Skelton, N. J., Ultsch, M. H., Santell, L., Dwyer, M. A., O'Connell, M. P. & Lazarus, R. A. (2000). *Nature (London)*, **404**, 465–470.
Eigenbrot, C., Kirchhofer, D., Dennis, M. S., Santell, L., Lazarus, R. A., Stamos, J. & Ultsch, M. H. (2001). *Structure*, **9**, 627–636.
Higashi, S., Nishimuraf, H., Aital, K. & Iwanaga, S. (1994). *J. Biol. Chem*. **269**, 18891–18898.
Kadono, S., Sakamoto, A., Kikuchi, Y., Oh-eda, M., Yabuta, N., Koga, T., Hattori, K., Shiraishi, T., Haramura, M., Kodama, H., Esaki, T., Sato, H., Watanabe, Y., Itoh, S., Ohta, M. & Kozono, T. (2004). *Biochem. Biophys. Res. Commun.* **324**, 1227–1233.
Kadono, S., Sakamoto, A., Kikuchi, Y., Oh-eda, M., Yabuta, N., Koga, T., Hattori, K., Shiraishi, T., Haramura, M., Kodama, H., Ono, Y., Esaki, T., Sato, H., Watanabe, Y., Itoh, S., Ohta, M. & Kozono, T. (2005). *Acta Cryst.* F**61**, 169–173.
Kadono, S., Sakamoto, A., Kikuchi, Y., Oh-eda, M., Yabuta, N., Yoshihashi, K. *et al.* (2005). *Biochem. Biophys. Res. Commun.* **327**, 589–596.
Kemball-Cook, G., Johnson, D. J., Tuddenham, E. G. & Harlos, K. (1999). *J. Struct. Biol.* **127**, 213–223.
Klingler, O., Matter, H., Schudok, M., Bajaj, S. P., Czech, J., Lorenz, M., Nestler, H. P., Schreuder, H. & Wildgoose, P. (2003). *Bioorg. Med. Chem. Lett.* **13**, 1463–1467.
Klingler, O., Schudok, M., Zoller, G., Heinelt, U., Defossa, E., Matter, H. & Safar, P. (2002). United States Patent US 6 500 803.
Kohrt, J. T. *et al.* (2005). *Bioorg. Med. Chem. Lett.* **15**, 4752–4756.
Kotian, P. L., Raman, K., Rowland, S., El-Kattan, Y., Saini, S. K., Dehghani, A., Upshaw, R., Bantia, S., Arnold, S., Babu, Y. S. & Chand, P. (2007). Submitted.
Lazarus, R. A., Olivero, A. G., Eigenbrot, C. & Kirchhofer, D. (2004). *Curr. Med. Chem.* **11**, 2275–2290.
Lovell, S. C., Davis, I. W., Arendall, W. B. III, de Bakker, P. I. W., Word, J. M., Prisant, M. G., Richardson, J. S. & Richardson, D. (2003). *Proteins*, **50**, 437–450.
Parlow, J. J., Case, B. L., Dice, T. A., Fenton, R. L., Hayes, M. J., Jones, D. J., Neumann, W. L., Wood, R. S., Lachance, R. M., Girard, T. J., Nicholson, N. S., Clare, M., Stegeman, R. A., Stevens, A. M., Stallings, W. C., Kurumbail, R. G. & South, M. S. (2003). *J. Med. Chem.* **46**, 4050–4062.

Parlow, J. J., Dice, T. A., Lachance, R. M., Girard, T. J., Stevens, A. M., Stegeman, R. A., Stallings, W. C., Kurumbail, R. G. & South, W. C. (2003). *J. Med. Chem.* **46**, 4043–4049.
Parlow, J. J., Kurumbail, R. G., Stegeman, R. A., Stevens, A. M., Stallings, W. C. & South, M. S. (2003*a*). *J. Med. Chem.* **46**, 4696–4701.
Parlow, J. J., Kurumbail, R. G., Stegeman, R. A., Stevens, A. M, Stallings, W. C. & South, M. S. (2003*b*). *Bioorg. Med. Chem. Lett.* **13**, 3721–3725.
Parlow, J. J., Stevens, A. M., Stegeman, R. A., Stallings, W. C., Kurumbail, R. G. & South, M. S. (2003). *J. Med. Chem.* **46**, 4297–4312.
Petersen, L. C., Bjorn, S. E., Nordfang, O., Norris, F. & Norris, K. (1996). *Eur. J. Biochem.* **235**, 310–316.
Pflugrath, J. W. (1999). *Acta Cryst.* D**55**, 1718–1725.
Pike, A. C., Brzozowski, A. M., Roberts, S. M., Olsen, O. H. & Persson, E. (1999). *Proc. Natl Acad. Sci. USA*, **96**, 8925–8930.
Rowland, S. (2002). *Curr. Opin. Drug Discov. Devel.* **5**, 613–619.
South, M. S., Dice, T. A., Girard, T. J., Lachance, R. M., Stevens, A. M., Stegeman, R. A., Stallings, W. C., Kurumbail, R. G. & Parlow, J. J. (2003). *Bioorg. Med. Chem. Lett.* **13**, 2363–2367.
Stagnitti, M. N. (2006). *Statistical Brief #109.* Agency for Healthcare Research and Quality, Rockville, MD, USA.
Szalony, J. A., Taite, B. B., Girard, T. J., Nicholson, N. S. & LaChance, R. M. (2002). *J. Thromb. Thrombolysis*, **14**, 113–121.
Zhang, E., St Charles, R. & Tulinsky, A. (1999). *J. Mol. Biol.* **285**, 2089–2104.
Zhu, B.-Y. & Scarborough, R. M. (2000). *Annu. Rep. Med. Chem.* **35**, 83–102.